

Design of Bipolar Differential OpAmps with Unity Gain Bandwidth up to 23 GHz

A. Budyakov^{1,2}, K. Schmalz², N.N. Prokopenko¹, C. Scheytt², P. Ostrovskyy²

¹ South Russia State University of Economics and Service, Radiotechnic Department,
Str. Shevchenko 147, 346500 Shakhty, Rostov region, Russia

alexbbster@gmail.com, budyakov@ihp-microelectronics.com, prokopenko@sssu.ru

² IHP, Im Technologiepark 25, 15236 Frankfurt/Oder, Germany
schmalz@ihp-microelectronics.com

Abstract— We compare the RF performance of fully differential opamps developed in 0.25 μm SiGe complementary (pnp/npn) technology and 0.13 μm SiGe BiCMOS (with npn only). Using the same compensation technique, the frequency response of these opamps is analyzed with emphasis on the phase margin (PM) and gain margin (GM). The pnp/npn opamp has advantage in unity gain bandwidth (UGB) and current consumption in comparison to the 0.13 μm BiCMOS design (supply voltage of 4V). For the pnp/npn opamp a 23 GHz UGB can be achieved with PM of 57 degrees. In case of the pnp/npn opamp the supply voltage can be reduced to 3V using a new topology with resistor for tail current. The optimized RF pnp/npn opamp allows the design of a differential line driver (50 Ohm) with 24 GHz bandwidth and a second order 2GHz biquad bandpass filter.

I. INTRODUCTION

Operational amplifiers (opamp) have moved to RF circuit design recently [1,2]. They can be used to design amplifiers, filters, signal conditioning circuits and line drivers. Fully differential opamps are especially attractive, because of their immunity to in-phase interference, increased dynamic range and reduced even-order harmonics. The design of an opamp for GHz range applications (RF opamp) requires very high transit frequency of the transistors because of stability problems, especially in applications with maximum negative feedback factor. To get the highest unity gain bandwidth (UGB) for a given technology, it is needed to minimize the number of transistors that process the signal from the input to the output of the opamp, that means to use a minimal “electrical length” (EL) circuits.

The influence of a transistor phase excess on phase margin of RF opamp is discussed in Section II. A comparison of RF opamps with supply voltage of 4V based on a BJT input stage (pnp/npn RF opamp) and a MOS-BJT cascode input stage (BiCMOS RF opamp) is presented in Section III. A new pnp/npn RF opamp topology for a 3V supply voltage is described in Section IV. Applications of an optimized pnp/npn

RF opamp for a 2GHz biquad bandpass filter and for a differential line driver are given in Section V.

II. INFLUENCE OF DELAY ON PHASE MARGIN

Accuracy of signal conditioning in an opamp depends on the open loop gain. The open loop gain of an opamp with one pole frequency response can be approximated at high frequency (from first pole frequency to UGB frequency) as follows:

$$A(f_s) = \frac{UGB}{f_s}, \quad (1)$$

where f_s is the signal frequency.

Further, accuracy of signal conditioning in RF applications depends mainly on UGB, because most of the spectra of the signal are usually located at RF frequency range. Thus, one can sacrifice DC open loop gain for UGB using minimal “electrical length” circuit of the RF opamp.

Let’s consider an opamp with two pole transfer function, where EL is the number of transistors taking part in signal processing, from the input to the output, and $\omega_T = 2\pi f_T$ is the transit frequency:

$$A(s) = \frac{A_{dc}}{(1 + s/\omega_{p1})(1 + s/\omega_{p2})} \cdot e^{-s \cdot EL / \omega_T} \quad (2)$$

Here A_{dc} is the DC open loop gain; ω_{p1} , ω_{p2} are the first and second pole frequencies.

The phase margin (PM) of an RF opamp with this transfer function was simulated (see fig.1) in SPICE with typical parameters; $A_{dc} = 200$ V/V, $\omega_{p1} = 2\pi \cdot 100 \cdot 10^6$ rad/s, $\omega_{p2} = 2\pi \cdot 30 \cdot 10^9$ rad/s, $\omega_T = 2\pi \cdot 150 \cdot 10^9$ rad/s.

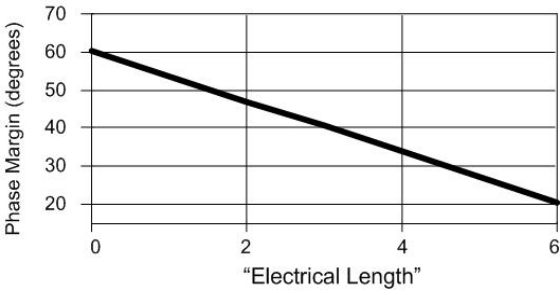


Figure 1. Phase margin of an opamp versus “electrical length” (EL) of the opamp

As fig.1 shows, the PM of the opamp degrades with increasing of EL. Therefore, it is important to design opamp topologies with minimal “electrical length” circuits, and compare the possible topologies.

III. COMPARISON PNP/NPN WITH BICMOS RF OPAMP

Optimal topologies for RF opamp with maximum negative feedback factor are circuits having a minimal number of transistors in the signal processing path, such as the circuits shown in figs.2a,b. The 0.13 μ m BiCMOS opamp shown in fig.2a was reported in [3,4]. We compare this RF opamp with the pnp/npn RF opamp in fig.2b. The RF opamp of fig.2b consists of a differential npn transistors (Q3 and Q6) input stage with pnp transistor load (Q2, Q5). The common mode feedback circuit (Q9, Q4) is the same as in fig.2a. The output voltage followers Q8 and Q11 provide a low output impedance and appropriate DC voltage level (2V) to drive an identical opamp input stage. This opamp has the minimal possible “electrical length”, but still enough DC open loop gain due to the high output impedance of the pnp active loads Q2, Q5. The opamp in fig.2b is based on a 0.25 μ m SiGe complementary technology [5] (pnp transistors with $f_T=85\text{GHz}$, $f_{\max}=120\text{GHz}$ and $BV_{\text{CEO}}=2.5\text{V}$, npn transistors with $f_T=170\text{GHz}$, $f_{\max}=170\text{GHz}$ and $BV_{\text{CEO}}=1.9\text{V}$). The simulation of the opamp in fig.2a is based on a 0.13 μ m SiGe BiCMOS (with npn only) technology, npn transistors have $f_T=170\text{GHz}$, $f_{\max}=170\text{GHz}$ and $BV_{\text{CEO}}=1.9\text{V}$ (preliminary data for SG13B [6]).

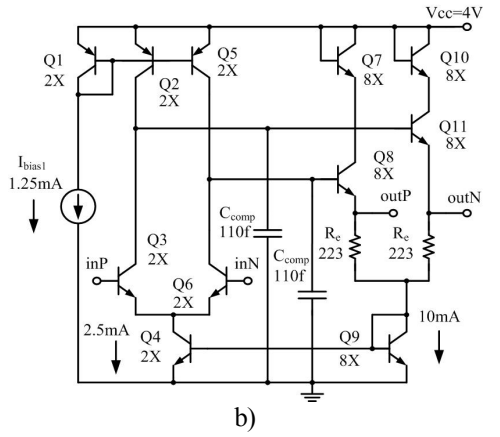
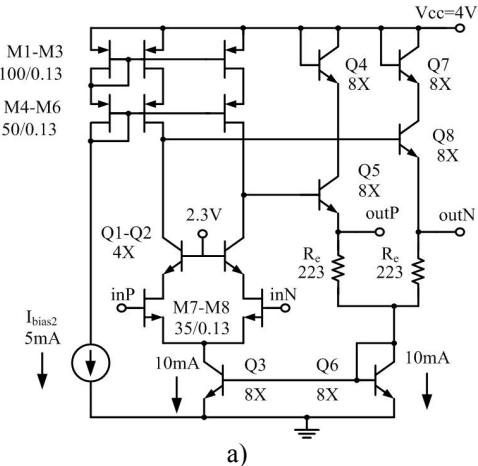


Figure 2. BiCMOS opamp (a) and pnp/npn opamp (b) circuits

For stable operation of an opamp with feedback, the equivalent second pole frequency of the opamp should be larger than the unity gain bandwidth frequency [7]. The second pole frequency of the opamps in figs.2a,b is defined by a time constant which is the product of the output resistance of signal source and the input capacitance of opamp.

The input capacitance of the pnp/npn opamp is dominated by the emitter-base diffusion capacitance of transistors Q3 and Q6 at frequencies close to UGB. A rough approximation of this capacitance is given by [7]:

$$C_{\text{inp.bip}} \approx \tau_b \frac{I_e}{V_T}, \quad (9)$$

where τ_b is the base transit time of Q3, Q6; I_e is the emitter DC current of Q3, Q6, $V_T \approx 26\text{mV}$ is the thermal voltage.

The input capacitance of the BiCMOS opamp, see fig.2a, is defined by the gate-source capacitance of M7, M8 and is proportional to the area ($A = W \times L$) of these transistors.

Thus, optimization of the second pole location can be performed by means of the DC collector bias current of the input stage in case of BJT input stage or the width of the input transistors in case of MOSFET input stage. The main simulated parameters of these opamps are given in table 1.

TABLE I. RF OPAMP PARAMETERS

RF opamp	Parameters and Units				
	SE UGB, GHz	PM, degrees	GM dB	DC Gain, dB	Iq, mA
pnp/npn	10.7	70	-15.5	39.4	12.5
BiCMOS	10.7	87	-7.6	30.8	20

To compare the parameters for these two opamps, we have designed them with an equal single ended UGB (SE UGB). The simulation results are depicted in fig.3.

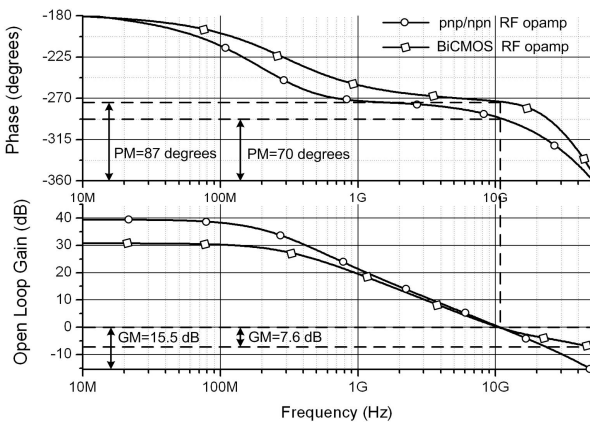


Figure 3. Simulated frequency responses of the opamps in fig.2a,b

The BiCMOS RF opamp has better phase margin, but the gain margin (GM) is worse compared to the pnp/npn RF opamp.

The PM of the pnp/npn RF opamp is smaller due to the effect of loading with the capacitance C_{comp} decreases the second pole frequency for higher C_{comp} and lower input stage transconductance [7]. At frequency higher than UGB, the roll-off of the phase characteristic for the BiCMOS RF opamp is higher, because of more transistors in the signal path (EL) compared to the pnp/npn RF opamp.

IV. LOW VOLTAGE TOPOLOGY OF PNP/NPN RF OPAMP

The supply voltage of the RF opamps in figs.2a,b is restricted to 4V due to the voltage headroom of the tail current sources, Q3 (fig.2a) and Q4 (fig.2b). If the emitter-collector voltage on these transistors is less than 0.7V, the output resistance is decreased, and saturation becomes possible.

The supply voltage of an opamp can be reduced using a resistor tail current, but then the common-mode rejection ratio drops drastically. Therefore, a new topology of a fully differential pnp/npn RF opamp (fig.4) was developed, which is based on circuit design ideas in [8].

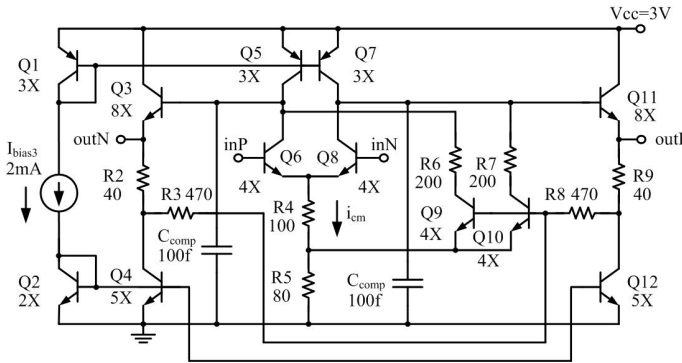


Figure 4. Low voltage fully differential pnp/npn RF opamp with resistor as the tail current

The bias conditions for Q6 and Q8 are:

$$I_{c6} \approx 0.5 \cdot I_{c4} \frac{R_2}{R_4}, \quad I_{c8} \approx 0.5 \cdot I_{c12} \frac{R_2}{R_4}. \quad (6)$$

Input and output common-mode voltages were simulated for the opamp, see fig.5 (the opamp was configured with DC feedback factor of unity and AC feedback factor of zero). To analyze the common mode operation, we consider a simplified equivalent circuit for the common mode input signal, see fig.5 on the right.

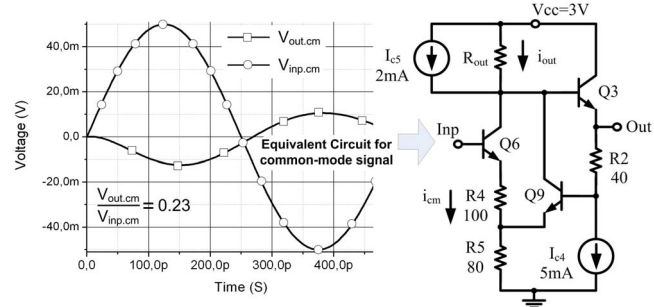


Figure 5. Input and output common-mode voltages in the low voltage pnp/npn RF opamp and its equivalent half circuit for common-mode signal

The Q6 collector current (i_{cm}) caused by the input common-mode voltage (Inp) is:

$$i_{cm} = V_{inp} / (R_4 + R_5 \parallel r_e). \quad (9)$$

The output current of the input stage is:

$$i_{out} = i_{cm} (1 - \alpha \frac{R_5}{r_e + R_5}), \quad (10)$$

where α is the emitter current gain of Q9, and r_e is the differential emitter-base junction resistance of Q9.

Hence, the output voltage (Out) in fig.5 is:

$$V_{out} = V_{inp} \frac{R_{out} \left(1 - \alpha \frac{R_5}{r_e + R_5} \right)}{R_4 + R_5 \parallel r_e}. \quad (11)$$

If the opamp is designed such that $\alpha \frac{R_5}{r_e + R_5} \approx 1$, the output voltage in fig.5 as well as the common-mode output voltage in fig.4 is close to zero.

Simulation results with layout parasites show the single-ended UGB is 8.7 GHz, while the differential one is 17.4 GHz (obtained by adding 6 dB to the simulated gain) with PM of 67 degrees. The differential output voltage swing is 890 mVp-p. The area of the opamp layout is 110 μ m \times 120 μ m without pads.

V. APPLICATIONS OF THE PNP/NPN RF OPAMP

Using the opamp topology given in fig.2b the pnp/npn opamp has been designed for maximum UGB with PM of 57 degrees. The parameters of the components are given in fig.6. The simulated frequency response of the opamp is shown in fig.7. The single-ended UGB is 12.3 GHz, while the differential one is 23 GHz. The area of the opamp layout is 110 μ m \times 130 μ m without pads.

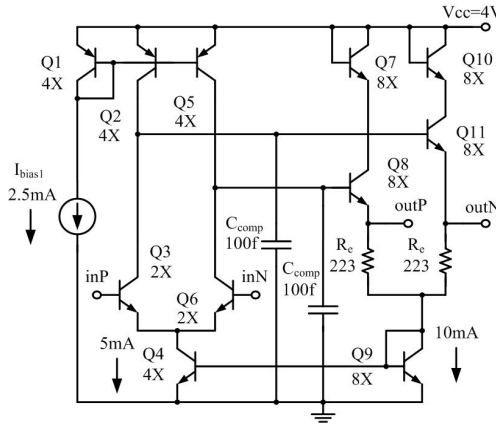


Figure 6. Pnp/npn RF opamp optimized for maximum UGB

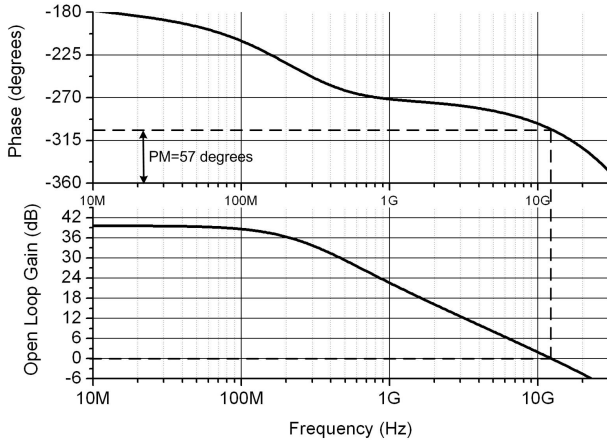


Figure 7. Simulated frequency response of the optimized pnp/npn RF opamp

A 50 Ohm line driver (fig.8) was designed using this RF opamp. The driver in fig.8 is an inverting opamp configuration with output resistors R_O for matching to a 50 Ohm load. The feedback resistors R_F and R_G are minimized to avoid degradation of the bandwidth, but input return loss starts to degrade at lower frequency in this case, compared to the classical line driver circuit [9]. The bandwidth of the driver is 24 GHz while input/output return losses are less -20 dB up to frequency of 2GHz. The OP_{1dB} is -3.2 dBm at 100 MHz for power gain of 0.6 dB. The differential noise figure of the driver is 12.5 dB up to 12 GHz.

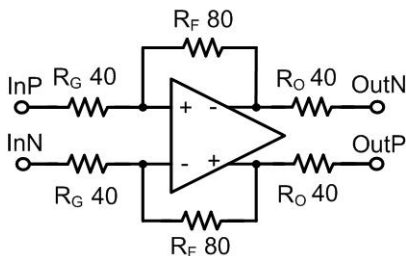


Figure 8. Line driver circuit

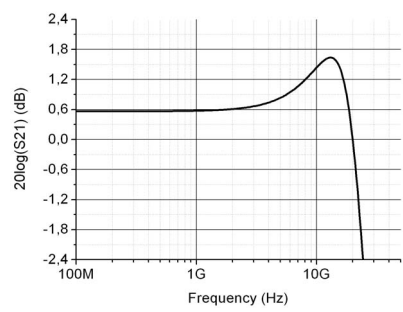


Figure 9. Simulated frequency response of the line driver

A biquad bandpass filter [9] was also designed with this opamp. The simulated input/output return losses of the filter are less -17 dB in the range 1GHz-3GHz, and IP_{1dB} and OP_{1dB} are -7dBm and -4.3dBm respectively. The differential noise figure of the filter is 21.6 dB at 2 GHz. The area of the filter layout is 0.6mmx0.6mm including pads.

VI. CONCLUSIONS

A design methodology for RF opamps has been presented. It was shown, that an RF opamp with unity gain bandwidth of 23 GHz can be realized in a SiGe complementary technology at 4 V supply voltage with PM of 57 degrees. Applications of this RF opamp were demonstrated for a 2 GHz bandpass biquad filter and a line driver with bandwidth of 24 GHz. A circuit design approach for RF opamp with 3 V supply voltage has been developed and implemented in a 0.25 μ m SiGe complementary technology.

ACKNOWLEDGMENT

We would like to thank Samiran Halder for discussion of the paper. This work was funded by Russian Federal Agency on Education within Russian President Grant for study abroad and IHP GmbH.

REFERENCES

- [1] Bruce Carter, "Using high-speed op amps for high-performance RF design, Part 1", (2Q 2002), <http://focus.ti.com/lit/an/slyt121/slyt121.pdf>
- [2] Bruce Carter, "Using high-speed op amps for high-performance RF design, Part 2", (3Q 2002), <http://focus.ti.com/lit/an/slyt112/slyt112.pdf>
- [3] S.P. Voinescu, et al., "Design Methodology and Applications of SiGe BiCMOS Cascode Opamps with up to 37-GHz Unity Gain Bandwidth," IEEE CSICS, Techn. Digest, pp.283-286, Nov. 2005.
- [4] S.P. Voinescu, et al., "SiGe BiCMOS for Analog, High-Speed Digital and Millimetre-Wave Applications Beyond 50 GHz," IEEE BCTM, pp.1-8, Oct.2006.
- [5] B. Heinemann et al. "Complementary SiGe BiCMOS", Electrochemical Society Proceeding, vol. 2004-07, pp.25-31.
- [6] Internal IHP GmbH report.
- [7] D. Johns and K. Martin, "Analog Integrated Circuit Design," John Wiley & Sons, 1997, pp.232-240, pp.50-61 and pp.154-156.
- [8] N.N. Prokopenko et al., "Architecture and Circuit Engineering of Precision Deferential Amplifiers with Increased Common-Mode Rejection", Proc. IEEE ICCSC, July 2006, pp.159-164.
- [9] Texas Instruments Application Note SLOA064, "A Differential Op-Amp Circuit Collection," (July, 2001), <http://focus.ti.com/lit/an/sloa064/sloa064.pdf>